Mon. Not. R. Astron. Soc. **325,** 1463–1470 (2001)

Axisymmetric modes of rotating relativistic stars in the Cowling approximation

José A. Font,[1★] Harald Dimmelmeier,[1★] Anshu Gupta[2★] and Nikolaos Stergioulas[3★]

[1]*Max-Planck-Institut für Astrophysik Karl-Schwarzschild-Str. 1, D-85741, Garching, Germany*
[2]*Raman Research Institute C. V. Raman Avenue, Sadashivanagar, Bangalore 560080, India*
[3]*Department of Physics, Aristotle University of Thessaloniki, Thessaloniki 54006, Greece*

Accepted 2001 March 28. Received 2001 March 28; in original form 2000 December 29

ABSTRACT

Axisymmetric pulsations of rotating neutron stars can be excited in several scenarios, such as core collapse, crust- and core-quakes or binary mergers, and could become detectable in either gravitational waves or high-energy radiation. Here, we present a comprehensive study of all low-order axisymmetric modes of uniformly and rapidly rotating relativistic stars. Initial stationary configurations are appropriately perturbed and are numerically evolved using an axisymmetric, non-linear relativistic hydrodynamics code, assuming time-independence of the gravitational field (Cowling approximation). The simulations are performed using a high-resolution shock-capturing finite-difference scheme accurate enough to maintain the initial rotation law for a large number of rotational periods, even for stars at the mass-shedding limit. Through Fourier transforms of the time evolution of selected fluid variables, we compute the frequencies of quasi-radial and non-radial modes with spherical harmonic indices $l = 0$, 1, 2 and 3, for a sequence of rotating stars from the non-rotating limit to the mass-shedding limit. The frequencies of the axisymmetric modes are affected significantly by rotation only when the rotation rate exceeds about 50 per cent of the maximum allowed. As expected, at large rotation rates, apparent mode crossings between different modes appear. In addition to the above modes, several axisymmetric inertial modes are also excited in our numerical evolutions.

Key words: hydrodynamics – relativity – methods: numerical – stars: neutron – stars: oscillations – stars: rotation.

1 INTRODUCTION

The pulsations of rotating neutron stars are expected to be a source of detectable gravitational waves. Additionally, their excitation could become detectable by the emission of high-energy radiation. In particular, axisymmetric oscillations can be excited in a number of different astrophysical scenarios, namely: (i) after a core collapse leading to a supernova explosion (see e.g. Mönchmeyer et al. 1991; Zwerger & Müller 1997), (ii) during starquakes induced by the secular spin-down of a pulsar, (iii) after a large thermonuclear explosion in the crust of an accreting neutron star, (iv) during a core-quake caused by a large phase transition to, for example, strange quark matter (Cheng & Dai 1998) and (v) in the delayed collapse of the merged object in a binary neutron star merger (Ruffert, Janka & Schäfer 1996; Shibata & Uryu 2000). The observational detection of such pulsations will yield valuable information about the equation of state of relativistic stars (see Kokkotas, Apostolatos & Andersson 2001; see also Kokkotas & Schmidt 1999 for a recent review on oscillations of relativistic stars).

Numerical simulations of some of these scenarios are available and provide very detailed information of the dynamics of the neutron star pulsations. In particular, the axisymmetric core-collapse simulations of Mönchmeyer et al. (1991) and Zwerger & Müller (1997) revealed that, after the collapse and bounce of an iron core, the unshocked inner core (the proto-neutron star) oscillates with varying volume (radial and quasi-radial) and surface modes. The amplitude and frequency of these fluid modes (f and p modes) was found to depend on the kinetic energy of the inner core at bounce, the stiffness of the equation of state (EOS), and the central and average densities of the inner core. These authors found that the amplitude of the post-bounce oscillations is small for spherical models, being strongly damped through the emission of asymmetric pressure waves, in time-scales of the order of 1 ms. However, for rotating cores which bounce as a result of centrifugal

★E-mail: font@MPA-Garching.MPG.DE (JAF); harrydee@MPA-Garching.MPG.DE (HD); anshu@rri.res.in (AG); niksterg@astro.auth.gr (NS)

forces at subnuclear densities, much larger amplitudes are achieved (as large as 10 times the central density) and the damping time-scale becomes comparable to the oscillation time-scale ($\gtrsim$1 ms). Recently, Dimmelmeier, Font & Müller (2001) have developed a code to study axisymmetric core collapse in general relativity using the conformally flat metric approach (Wilson, Mathews & Marronetti 1996). This code is currently being applied to collapse some of the initial models of Zwerger & Müller (1997), to analyze the gravitational waves emitted in the process. Excitation of axisymmetric modes have already been observed in such relativistic core-collapse simulations.

Of all axisymmetric modes, the quasi-radial modes of slowly-rotating relativistic stars were first studied by Hartle & Friedman (1975) and, more recently, by Datta et al. (1998). In rapid rotation, quasi-radial modes of relativistic stars have been studied by Yoshida & Eriguchi (2001) in the Cowling approximation (McDermott, Van Horn & Scholl 1983), i.e. by neglecting the perturbations in the gravitational field (see Stergioulas 1998 for a recent review on the equilibrium structure and oscillations of rapidly rotating stars in general relativity). For Newtonian stars, axisymmetric modes have been extensively studied by Clement (1981, 1984, 1986). From the studies mentioned above, it has become apparent that rotation not only weakly modifies the oscillation frequencies for low-order modes, but also introduces apparent crossings between higher-order modes for rapidly rotating models. In addition, in Clement (1981) it is claimed that the axisymmetric quadrupole f mode lies on a continuous branch for rapidly rotating Newtonian stars.

In this paper we compute all low-order $l = 0$, 1, 2 and 3 axisymmetric modes for rapidly rotating stars in general relativity, in the Cowling approximation. For this purpose, we use a 2D non-linear hydrodynamics code, the accuracy of which has been extensively tested in Font, Stergioulas & Kokkotas (2000) (hereafter FSK; see also Stergioulas, Font & Kokkotas 2000). This code is based on high-resolution shock-capturing (HRSC) finite-difference schemes for the numerical integration of the general relativistic hydrodynamic equations (see Font 2000 for a recent review). We note in passing that the 3D version of the numerical methods employed here has been applied recently by Stergioulas & Font (2001) in the study of the large-amplitude, non-linear evolutions of r modes in rotating relativistic stars. In our present study of axisymmetric modes, we focus on a sequence of equilibrium models with a polytropic ($N = 1.0$) EOS and uniform rotation. For the excitation of the various oscillation modes, low-amplitude perturbations (using appropriate trial eigenfunctions) are added to the initial equilibrium models. The Cowling approximation allows us to evolve relativistic matter for a much longer time than the presently available coupled space–time plus hydrodynamical evolution codes (Alcubierre et al. 2000; Font et al. 2000; Shibata, Baumgarte & Shapiro 2000; Shibata & Uryu 2000). This is particularly evident when hydrodynamically evolving rotating stars. Nevertheless, because pulsations of neutron stars are a mainly hydrodynamical process, the approximation of a time-independent gravitational field still allows for qualitative conclusions to be drawn when studying the evolution of perturbed rotating neutron stars. In addition, our present results will serve as test-beds for 3D general-relativistic evolution codes.

The paper is organized as follows. In Section 2 we describe the set-up of the problem by briefly presenting some details of the initial equilibrium stellar configurations and the main features of the hydrodynamical code. In Section 3 we explain the procedure by which the initial equilibrium models are perturbed. Section 4 presents the main results of our simulations, including the frequencies of all low-order axisymmetric modes for our sample of initial models. The paper ends with Section 5, where a summary is presented together with an outlook of possible future directions of this investigation.

2 PROBLEM SET-UP

Our initial models are numerical solutions of the exact equations that describe rapidly rotating relativistic stars that have uniform angular velocity Ω. We assume a perfect fluid, zero-temperature EOS, for which the energy density is a function of pressure only. The following relativistic generalization of the Newtonian polytropic EOS is chosen:

$$p = K\rho_0^{1+1/N}, \tag{1}$$

$$\epsilon = \rho_0 + Np, \tag{2}$$

where p is the pressure, ϵ is the energy density, ρ_0 is the rest-mass density, K is the polytropic constant and N is the polytropic exponent. The initial equilibrium models are computed using a numerical code developed by Stergioulas & Friedman (1995). Our representative neutron star models are characterized by $N = 1$, $K = 100$ and central density $\rho_c = 1.28 \times 10^{-3}$, in units of $c = G = \mathrm{M}_\odot = 1$. We compute 12 different initial models by varying the polar to equatorial circumferential radius from 1 (non-rotating star) to 0.65 (near the mass-shedding limit), as listed in Table 1. The angular velocity at the mass-shedding limit is $\Omega_K = 0.5363 \times 10^4\ \mathrm{s}^{-1}$ for this sequence of rotating relativistic stars of same central density. In order to be able to study stellar pulsations, the initial model is supplemented by a uniform, non-rotating 'atmosphere' of very low density, typically 10^{-6} or less times the central density of the star (see related discussion in FSK).

The initial data are subsequently evolved in time with a hydrodynamics code. The (axisymmetric) hydrodynamic equations are written as a first-order flux-conservative system that expresses the conservation laws of mass, momentum and energy. The specific form of the equations was presented in FSK and we will not repeat it here. These equations are solved using a HRSC finite-difference

Table 1. Equilibrium properties of the initial models, as described by a polytropic EOS, $p = K\rho_0^{1+1/N}$, where $N = 1$, $K = 100$ and with central rest-mass density $\rho_c = 1.28 \times 10^{-3}$ (in units with $c = G = \mathrm{M}_\odot = 1$). The entries in the table are as follows: Ω is the angular velocity of the star, M and M_0 are the gravitational and rest mass, T/W is the ratio of rotational to gravitational binding energy and R is the equatorial circumferential radius.

Ω ($10^4\ \mathrm{s}^{-1}$)	M ($\mathrm{M}_\odot$)	M_0 ($\mathrm{M}_\odot$)	T/W ($\times 10^{-2}$)	R (km)
0.0	1.400	1.506	0.0	14.15
0.218	1.432	1.541	1.200	14.51
0.306	1.466	1.579	2.438	14.92
0.371	1.503	1.619	3.701	15.38
0.399	1.523	1.641	4.339	15.63
0.423	1.543	1.663	4.976	15.91
0.445	1.564	1.686	5.609	16.21
0.465	1.585	1.709	6.232	16.52
0.482	1.607	1.733	6.839	16.87
0.498	1.627	1.756	7.419	17.25
0.511	1.647	1.778	7.959	17.68
0.522	1.666	1.798	8.439	18.15

scheme (Font 2000). A comprehensive description of the specific numerical techniques that we employ was previously reported in FSK. Therefore, we only mention here that the code makes use of the third-order piecewise parabolic method (PPM; Colella & Woodward 1984), for the cell-reconstruction procedure, together with Marquina's flux formula (Donat et al. 1998) to compute the numerical fluxes. The PPM reconstruction scheme was shown to be accurate enough for maintaining the initial rotation laws during many rotational periods.

The hydrodynamic equations are implemented in the code using the spherical polar coordinates (r, θ, ϕ) and assuming axisymmetry, i.e. all derivatives with respect to the ϕ coordinate vanish. The radial computational domain extends to 1.2 times the radius of the star (the 20 per cent additional zones are used for the atmosphere). In the polar direction, the selected domain depends on the spherical harmonic index of the pulsation modes: for even l modes the domain extends from $\theta = 0$ (pole) to $\theta = \pi/2$ (equator), while for odd l modes the domain extends to $\theta = \pi$. The number of grid points we employ is 200×80 for l being even and 160×120 for l being odd, in r and θ respectively. The boundary conditions are implemented in the same way as in FSK.

Our numerical evolution code was thoroughly tested in FSK, by comparing evolutions of perturbed spherical stars with results from perturbation theory obtained with an independent eigenvalue code. Since then, the code has been upgraded to run efficiently on a NEC SX-5/3C vector supercomputer. This modification was essential for doing a large number of numerical evolutions for many rotational periods and with a large number of grid-points.

3 PERTURBATION OF THE INITIAL DATA

The accurate computation of mode frequencies in a rotating star requires an appropriate excitation of the equilibrium initial data. When doing so, it is possible to obtain the frequencies of the excited modes with good accuracy, through a Fourier transform of the time evolution of the hydrodynamical variables, provided that the evolution time is much larger than the period of oscillations. As in the hydrodynamical evolution, we are using the 3+1 formulation (Banyuls et al. 1997), the oscillation frequencies of the various evolved variables are obtained with respect to the coordinate time at a given location. This corresponds to the frequency of oscillations in a reference frame attached to an inertial observer at infinity. To increase accuracy in the computation of the frequencies, we search for the zeros of the first derivative of the Fourier transform (with respect to the frequency), using second-order accurate central differences. These zeros correspond to maxima in the Fourier transform, which (except for high-frequency noise) correspond to the excited modes of oscillation. This procedure is performed at several points inside the star and the frequencies thus determined are found to be the same for each mode, i.e. all the modes that we identify are global discrete modes. For the resolution employed we estimate the accuracy of the computed frequencies to be of the order of 1–2 per cent. The different pulsation frequencies are identified with specific normal modes by comparing frequencies of the non-rotating star to known eigenfrequencies from perturbative normal-mode calculations.

As demonstrated in FSK, the small-amplitude pulsations in the non-linear, fixed space–time evolutions correspond to linear normal modes of pulsation in the relativistic Cowling approximation (McDermott et al. 1983), in which perturbations of the space–time are ignored. The existence of a numerical viscosity, inherent to the numerical scheme, damps the pulsations of the star. Therefore, high-resolution grids are preferred to reduce the damping, especially for the higher frequency modes, which are damped faster. In addition, our numerical scheme requires the presence of a tenuous, constant-density 'atmosphere' surrounding the star, which is reset to its initial state after each time-step (in such a way that the stellar surface is allowed to contract or expand). This introduces an additional numerical damping of the pulsations, as a result of finite-differencing at the surface of the star. In order to minimize this effect, the density of the 'atmosphere' has to be small enough to be dynamically unimportant. As already mentioned, a typical value of $10^{-6}\rho_c$ is appropriate for this purpose.

We use analytic eigenfunctions to excite particular oscillation modes. For the $l = 0$ modes the initial equilibrium values of density and pressure, ρ_0 and p_0, are perturbed to non-equilibrium values, $\rho = \rho_0 + \delta\rho$ and $p = p_0 + \delta p$ by the eigenfunctions

$$\delta\rho = A\rho_c \sin\left[\frac{\pi r}{r_s(\theta)}\right], \tag{3}$$

$$\delta p = \Gamma p_i \frac{\delta\rho}{\rho_i}, \tag{4}$$

where ρ_c is the central density, $r_s(\theta)$ is the coordinate radius of the surface of the star (which depends on the polar angle θ) and Γ is the adiabatic index of the ideal gas EOS, $p = (\Gamma - 1)\rho\epsilon$, related to the polytropic index by the equation $\Gamma = 1 + 1/N$ (for isentropic stars). The amplitude of the excitation, A, is typically chosen to be in the range of 0.001 to 0.005.

For the excitation of the $l = 1$, 2 and 3 modes, we add a small non-zero θ-velocity component to perturb the initial vanishing value. More precisely, for $l = 1$ we have

$$v_\theta = A \sin\left[\frac{\pi r}{r_s(\theta)}\right] \sin\theta, \tag{5}$$

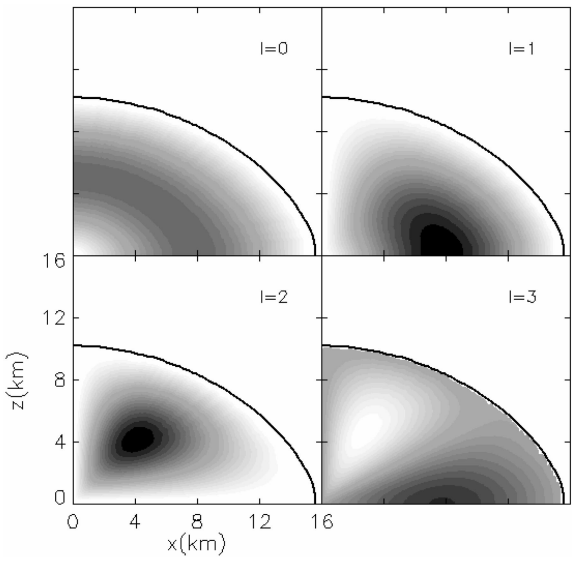

Figure 1. 2D grey-scale plot of the initial data used for mode-excitation: density perturbation ($l = 0$) and $v_\theta (l \neq 0)$. The darkest area corresponds to the maximum of the perturbation, while the lightest area corresponds to its minimum values. The thick solid line indicates the location of the surface of the star. The depicted initial model is the fastest rotator of our sample in Table 1.

for $l = 2$

$$v_\theta = A \sin\left[\frac{\pi r}{r_s(\theta)}\right] \sin\theta\cos\theta, \tag{6}$$

and for $l = 3$

$$v_\theta = A \sin\left[\frac{\pi r}{r_s(\theta)}\right] \sin\theta(1 - 5\cos^2\theta). \tag{7}$$

The particular radial dependence in the above eigenfunctions is chosen so that the perturbations vanish at the surface of the rotating star. We have found that this is necessary for our numerical scheme to work. Fig. 1 displays a 2D grey-scale plot of the above perturbations, for the model near the mass-shedding limit. The darkest area corresponds to the maximum of the perturbation, while the lightest area corresponds to its minimum values. We note that all models have equatorial plane symmetry with respect to the $z = 0$ axis, even though we use a grid extending to $\theta = \pi$ for odd l modes. The choice of these trial eigenfunctions allows us to compute the four lowest frequencies quite accurately for all the considered l modes, as we discuss next.

4 RESULTS

We turn now to presenting our numerical results concerning the frequencies of axisymmetric pulsations of uniformly and rapidly rotating neutron stars.

4.1 Quasi-radial modes

Fig. 2 shows the time evolution of the radial velocity component for the most rapidly rotating model in our sequence. The initial equilibrium model has been perturbed with an $l = 0$ perturbation according to equations (3) and (4). The final evolution time corresponds to 10 ms, and the oscillations are measured at half the radius of the star and at an angle of $\theta = \pi/4$. The oscillatory pattern depicted in this figure is typical to all our simulations: it is mainly a superposition of the lowest-order normal modes of the fluid. The amplitude of the oscillations is damped as a result of the inherent viscosity of the numerical scheme. The high-frequency normal modes are usually damped faster and at the final time the star is pulsating mostly in a few lowest frequency modes.

The frequencies of the axisymmetric modes are obtained by a fast Fourier transform of the time evolution of selected hydrodynamical variables (both the density and the components of the velocity). Fig. 3 shows the Fourier transform of the radial velocity evolution depicted in Fig. 2. The main mode which is excited is the fundamental quasi-radial F mode. Its higher harmonics ($H1$–$H3$) are also excited, as well as several other, non-radial modes. The amount of excitation of each mode depends on the correlation between the mode eigenfunction and the applied perturbation.

As it is apparent in Fig. 3, a dense spectrum of modes appears when one applies generic perturbations that do not correspond to the eigenfunctions of a particular normal mode only. Thus, in order to identify the peaks in the Fourier transform with specific normal modes, we rely on the previously known frequencies in the non-rotating limit (see FSK). As the rotation rate is increased, we follow the change in the location of the various peaks, keeping in mind that apparent crossings of frequencies occur at large rotation rates. In such a case, the amplitude of the Fourier transform at various points inside the star (which correlates with the mode eigenfunction) is used as a guide in deciding about the correct identification of the mode frequency. The specific values for the frequencies of the fundamental F and higher harmonics H_1, H_2, and H_3 quasi-radial modes for the sequence of rotating stars considered here, are shown in Table 2.

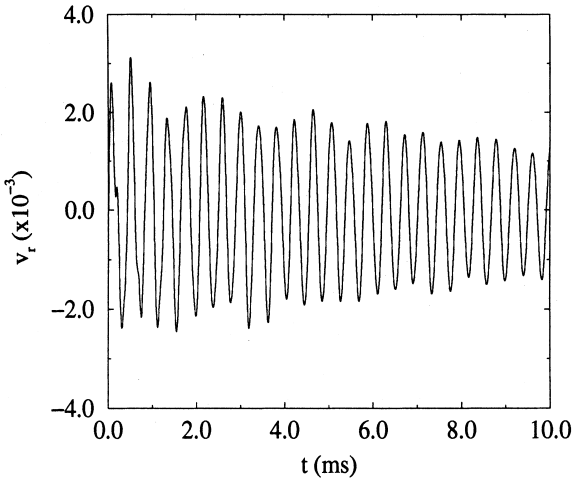

Figure 2. Time evolution of the radial velocity of the most rapidly rotating model of our sequence, $\Omega = 0.522 \times 10^4\ \mathrm{s}^{-1}$. An $l = 0$ perturbation has been applied to the equilibrium data. The pulsations are mainly a superposition of the normal modes of the star.

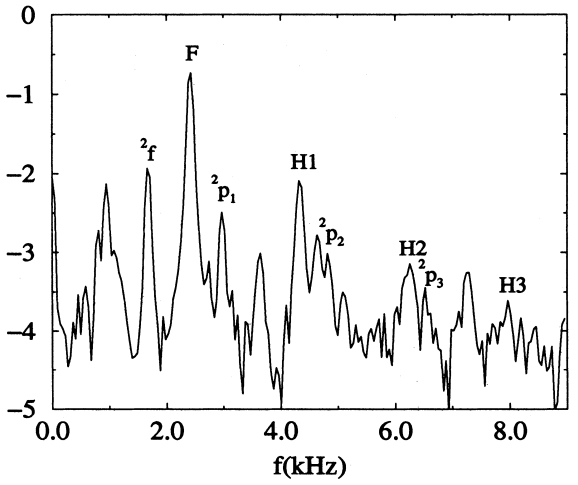

Figure 3. Logarithm of the amplitude (in arbitrary scale) resulting from the Fourier transform of the radial velocity evolution shown in Fig. 2. It is possible to identify in this plot the frequencies of the fundamental quasi-radial mode as well as up to three harmonics. Additionally, f and overtones of p modes can also be identified.

As frequencies of quasi-radial modes have been computed previously by Yoshida & Eriguchi (2001), as an eigenvalue problem, we use those results to compare the values obtained with our code for a soft polytrope with $\rho_c = 8.1 \times 10^{-4}$, $N = 1.5$ and $K = 4.349$. We have compared the models corresponding to $\Omega = 0, 7.1379 \times 10^{-3}$ and 1.4094×10^{-2}, which, in the notation of Yoshida & Eriguchi correspond to $f_{\rm rot} = 0$, 0.1415 and 0.2794, respectively. The results of this comparison are presented in Table 3. We note that the agreement is very good, especially for the most rapidly rotating model; the differences always being below 2 per cent. As there may be some small differences in the construction of the equilibrium model, the actual accuracy of our code is better than the relative differences shown in Table 3.

Table 2. Fundamental, first, second and third overtones (F, H_1, H_2 and H_3, respectively) of the quasi-radial ($l = 0$) modes for a sequence of rotating stars of same central density. The angular velocity Ω_K at the mass-shedding limit is $0.5363 \times 10^4\ s^{-1}$ for this sequence.

Ω ($10^4\ s^{-1}$)	F (kHz)	H_1 (kHz)	H_2 (kHz)	H_3 (kHz)
0.0	2.706	4.547	6.320	8.153
0.218	2.657	4.467	6.215	8.005
0.306	2.619	4.409	6.202	8.005
0.371	2.579	4.385	6.234	8.096
0.399	2.553	4.377	6.243	8.098
0.423	2.535	4.371	6.241	8.134
0.445	2.510	4.362	6.266	8.171
0.465	2.495	4.356	6.262	8.171
0.482	2.476	4.366	6.274	8.197
0.498	2.456	4.357	6.270	8.130
0.511	2.442	4.350	6.297	8.030
0.522	2.417	4.337	6.255	7.987

Table 3. Comparison of $l = 0$ quasi-radial pulsation frequencies, obtained with the present non-linear evolution code, to linear perturbation mode frequencies in the relativistic Cowling approximation (Yoshida & Eriguchi 2001). The equilibrium model is a $N = 1.5$, $K = 4.349$ relativistic polytrope with $\rho_c = 8.1 \times 10^{-4}$.

Ω (10^{-3})	Mode	Y&E (kHz)	present (kHz)	Difference (per cent)
0	F	1.674	1.678	0.3
	H1	2.758	2.807	1.7
	H2	3.793	3.841	1.3
7.1379	F	1.646	1.670	1.5
	H1	2.696	2.735	1.4
	H2	3.728	3.761	0.9
14.094	F	1.545	1.553	0.5
	H1	2.572	2.595	0.9
	H2	3.664	3.642	0.6

4.2 Non-radial modes

In Figs (4)–(9) we plot the time evolutions of the polar velocity component, along with the corresponding Fourier transforms for non-radial $l = 1$, 2 and 3 perturbations, for the fastest rotating model in Table 1. The time evolutions shown are measured at half the star radius and $\theta = 2\pi/3$ for $l = 1$ and 3, and $\theta = \pi/3$ for $l = 2$. The above time evolutions show the same qualitative behaviour already described for the $l = 0$ modes. The lowest frequency (and dominant) $l = 1$ mode we excite in our time evolutions (labelled ^{1}f) has no nodes along the radial direction and behaves like a fundamental mode. We point out that the $l = 1$ fundamental mode does not exist when one considers the full set of equations (i.e. including the perturbation of the metric), as a result of momentum conservation (it would correspond to a displacement of the centre of mass). In the Cowling approximation, however, momentum is not conserved, as the perturbation in the metric is neglected. In this approximation, only the fluid oscillates in a fixed background metric and an oscillation of the centre of mass is allowed, as the fixed metric acts as a restoring force.

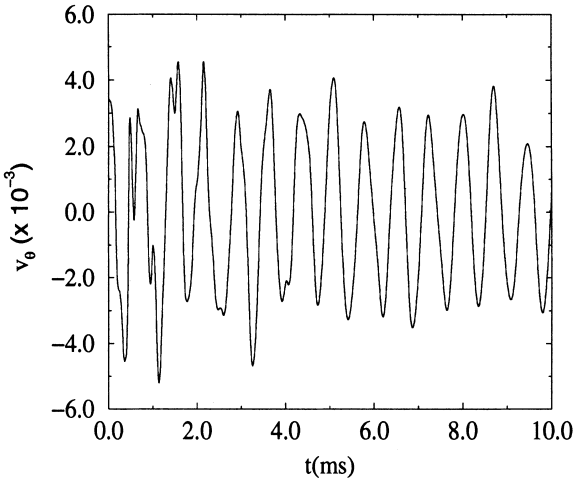

Figure 4. Time evolution of the polar velocity component for the fastest rotator, $\Omega = 0.522 \times 10^4\ s^{-1}$. An $l = 1$ perturbation has been applied to the equilibrium data.

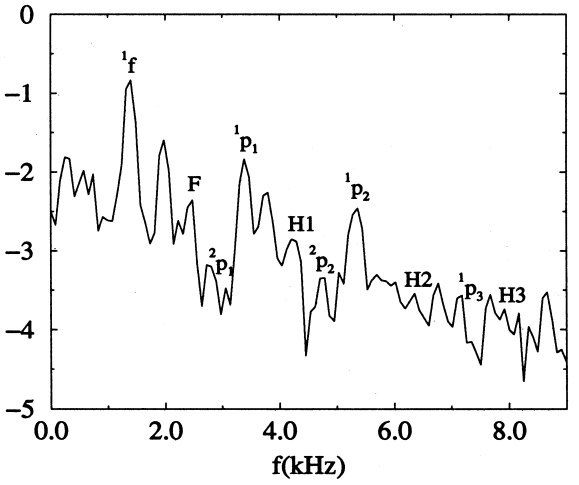

Figure 5. Fourier transform of the polar velocity evolution shown in Fig. 4. The different axisymmetric, $l = 1$ modes are conveniently labelled.

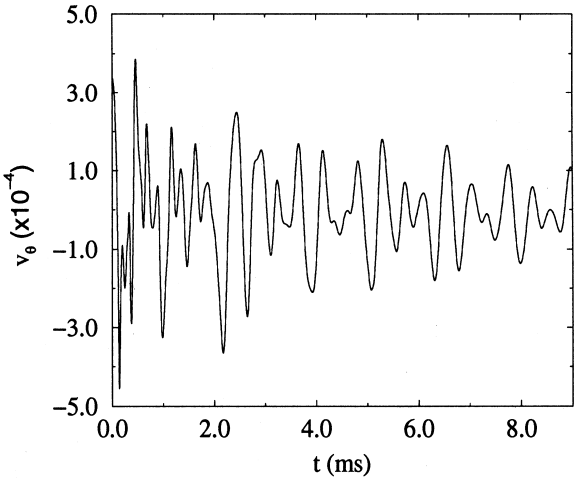

Figure 6. Same as Fig. 4 but showing the time evolution for the $l = 2$ perturbation.

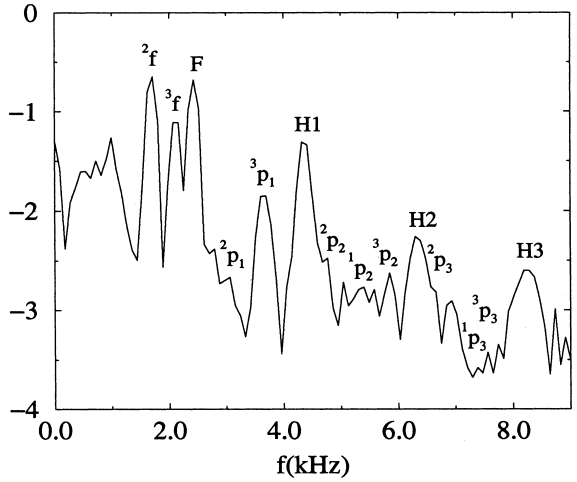

Figure 7. Same as Fig. 5 but showing the frequencies of the $l = 2$ axisymmetric modes.

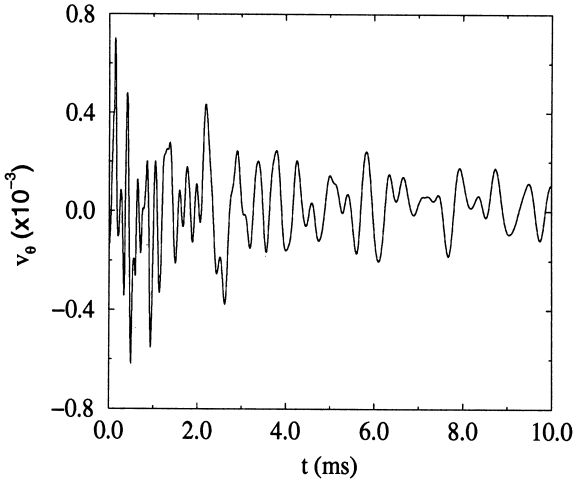

Figure 8. Same as Fig. 4 but showing the time evolution for the $l = 3$ perturbation.

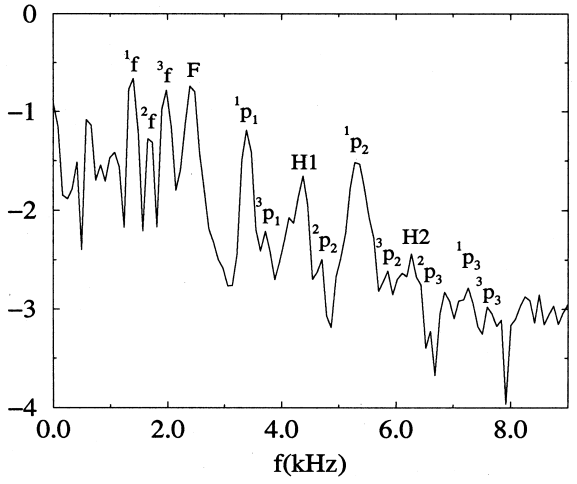

Figure 9. Same as Fig. 5 but showing the frequencies of the $l = 3$ axisymmetric modes.

For $l = 2$, a larger number of modes is excited by the initial perturbation. At late times, the evolution is mainly a superposition of the fundamental ^{2}f mode and the fundamental quasi-radial F mode, as it is evident from the amplitudes of the various modes in the corresponding Fourier transform.

For $l = 3$, a large number of modes is also excited by the initial perturbation, as in the $l = 2$ case. At late times, the evolution is mainly a superposition of the fundamental ^{3}f and ^{1}f modes and of the fundamental quasi-radial F mode. The Fourier amplitude of the ^{1}f mode is larger than the amplitude of the ^{3}f mode, which shows that the eigenfunction of the $l = 3$ modes near the mass-shedding limit is significantly modified by rotation, so that the $l = 3$ part of the ^{1}f eigenfunction correlates better with the generic eigenfunction we used to excite $l = 3$ modes than the ^{3}f eigenfunction itself.

The frequencies of all identified $l = 1$, 2 and 3 modes are displayed in detail in Tables 4–6. The modes are labelled as ^{l}f for the fundamental modes and ^{l}p$_n$ for the p modes of order n. A plot of all mode frequencies as a function of the rotation rate is shown in Fig. 10. At rotation rates below ~50 per cent of the mass-shedding limit, the frequencies of the lowest-order modes are not significantly affected by rotation. This is consistent with previous results in the slow-rotation approximation (Hartle & Friedman 1975) and in the Newtonian limit. For larger rotation rates, however, the $l = 0$ and $l = 1$ overtones have a tendency to increase in frequency with rotation rate, while the $l = 2$ and $l = 3$ overtones have the opposite tendency. As a result, several apparent mode crossings take place between different modes. This has been observed before by Clement (1986) for Newtonian axisymmetric modes and by Yoshida & Eriguchi (2001) for the relativistic quasi-radial modes.

In the above studies, when one follows an eigenfrequency continuously from the non-rotating limit to the large rotation rates, then, at apparent mode crossings, the continuous lines corresponding to different frequency sequences do not cross, which is normally called 'avoided crossing'. Such avoided crossings can occur in two ways: the eigenfunction along a continuous frequency sequence remains as that of the same mode (which is the usual type of avoided crossing in non-rotating stars, see Unno et al. 1989) or a different mode appears in the same continuous frequency sequence after the avoided crossing. The latter case is encountered in rotating stars, as in Fig. 10. To distinguish the two cases, we prefer to use the term 'apparent crossing' for rotating stars (as was done in Clement 1986), which refers to a mode-sequence, rather than a frequency sequence.

Finally, we note that in Clement (1981) it is claimed that the axisymmetric ^{2}f mode lies on a continuous branch, near the mass-shedding limit, for rapidly rotating Newtonian stars. In our relativistic computation, no such behaviour was found for any of the modes studied. Within the numerical resolution employed all the identified modes were found to be discrete.

4.3 Inertial modes

Apart from the quasi-radial and f and p modes, a number of axisymmetric inertial modes was also excited in our numerical evolutions, which can be seen as low-frequency peaks in our Fourier transforms (Figs 3–9). These modes exist in isentropic stars (such as those considered here) as a mixture of axial r modes and polar g modes (see Lockitch & Friedman 1999). Non-axisymmetric inertial modes have been computed as an eigenvalue problem for slowly rotating relativistic stars (Lockitch 1999; Lockitch, Andersson & Friedman 2001), but frequencies for

Table 4. The f mode and first three p modes corresponding to $l = 1$. Further details in Tables 1 and 2.

Ω ($10^4\,s^{-1}$)	^{1}f (kHz)	^{1}p$_1$ (kHz)	^{1}p$_2$ (kHz)	^{1}p$_3$ (kHz)
0.0	1.335	3.473	5.335	7.136
0.218	1.349	3.464	5.318	7.134
0.306	1.356	3.453	5.317	7.152
0.371	1.364	3.446	5.320	7.172
0.399	1.369	3.442	5.322	7.193
0.423	1.371	3.438	5.325	7.214
0.445	1.373	3.434	5.328	7.238
0.465	1.375	3.429	5.333	7.223
0.482	1.376	3.422	5.339	7.349
0.498	1.376	3.417	5.340	7.288
0.511	1.375	3.407	5.337	7.281
0.522	1.375	3.393	5.335	7.318

Table 5. The f mode and first three p modes corresponding to $l = 2$. Further details in Tables 1 and 2.

Ω ($10^4\,s^{-1}$)	^{2}f (kHz)	^{2}p$_1$ (kHz)	^{2}p$_2$ (kHz)	^{2}p$_3$ (kHz)
0.0	1.846	4.100	6.019	7.867
0.218	1.855	4.040	5.910	7.684
0.306	1.860	3.944	5.716	7.471
0.371	1.857	3.814	5.521	7.264
0.399	1.851	3.734	5.431	7.130
0.423	1.844	3.645	5.325	7.000
0.445	1.832	3.554	5.226	6.989
0.465	1.815	3.456	5.164	6.970
0.482	1.787	3.352	4.962	6.823
0.498	1.762	3.244	4.810	6.746
0.511	1.733	3.120	4.822	6.653
0.522	1.686	3.010	4.726	6.571

Table 6. The f mode and first three p modes corresponding to $l = 3$. Further details in Tables 1 and 2.

Ω ($10^4\,s^{-1}$)	^{3}f (kHz)	^{3}p$_1$ (kHz)	^{3}p$_2$ (kHz)	^{3}p$_3$ (kHz)
0.0	2.228	4.622	6.635	8.600
0.218	2.228	4.570	6.550	8.418
0.306	2.221	4.485	6.433	8.304
0.371	2.199	4.380	6.280	8.109
0.399	2.186	4.330	6.214	8.105
0.423	2.177	4.303	6.135	8.000
0.445	2.148	4.194	6.067	7.831
0.465	2.118	4.124	5.987	7.751
0.482	2.094	4.044	5.895	7.751
0.498	2.055	3.964	5.784	7.656
0.511	2.017	3.870	5.852	7.612
0.522	1.965	3.720	5.767	7.593

axisymmetric modes are not available yet. This makes their identification difficult, as, in our simulations, many modes with similar frequencies appear. Furthermore, the spacing between these frequencies is of the same order as one would expect the difference between the relativistic frequencies and the Newtonian frequencies (computed in Lockitch & Friedman 1999) to be. Therefore, it would be too venturous, at this point, to attempt an identification with specific normal modes without prior knowledge of some of these frequencies in relativity, at least for slow rotation.

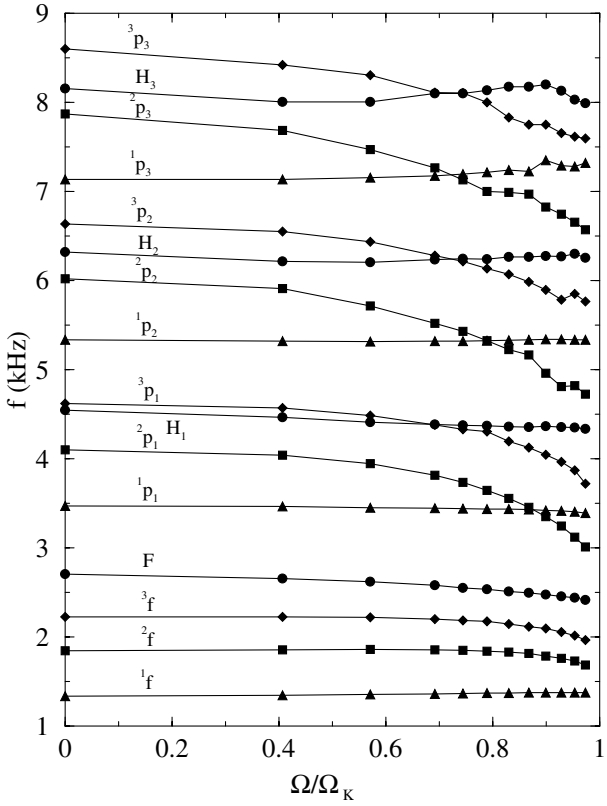

Figure 10. Frequencies of the lowest three quasi-radial modes versus the ratio of angular velocity of the star Ω to the angular velocity at the mass-shedding limit Ω_K, for the sequence of rotating relativistic stars in Table 1. This figure appears in colour in Synergy, the online version of MNRAS.

5 SUMMARY AND OUTLOOK

We have presented a comprehensive study of all low-order axisymmetric modes of uniformly and rapidly rotating relativistic stars in the Cowling approximation. This investigation has been carried out by numerically evolving initial perturbed equilibrium configurations with an axisymmetric, non-linear, relativistic hydrodynamics code. The simulations were performed using a high-resolution shock-capturing finite-difference scheme accurate enough to maintain the initial rotation law for a sufficient number of rotational periods.

Through Fourier transforms of the time evolution of selected fluid variables we computed the frequencies of non-radial, axisymmetric modes (with angular momentum indices $l = 0$, 1, 2 and 3) of rapidly rotating stars. Therefore, we have extended previous results by Yoshida & Eriguchi (2001), which were mainly restricted to quasi-radial modes. We have presented results for a complete sequence of rotating stars, ranging from the non-rotating case to rapid rotation near the mass-shedding limit. Apparent crossings between different modes appear for rapidly rotating stars, as a result of the different influence of rotation on quasi-radial and $l = 1$ modes than on modes with $l \geq 2$. This different behaviour may be related to the fact that the rotational deformation of the equilibrium star appears first as an $l = 2$ term. Several axisymmetric inertial modes were also excited in our simulations. However, a definitive identification of the observed frequency peaks with specific modes will only be possible when mode frequencies on the slow-rotation approximation be computed as an eigenvalue problem. Alternatively, a determination of mode

eigenfunctions in our simulations (and a comparison to mode eigenfunctions in the Newtonian limit) may also allow the identification of such inertial modes.

In following work we plan to study axisymmetric modes of differentially rotating stars with realistic equations of state. Moreover, the implementation of the hydrodynamic equations and numerical techniques employed in the present work has been recently extended (Dimmelmeier et al. 2001) to allow for gravitational field dynamics through the so-called *conformally flat metric* approach (Wilson et al. 1996). Studies of fully coupled evolutions with such a code, in the context of pulsations of rotating relativistic stars, will be presented elsewhere.

ACKNOWLEDGMENTS

We thank John Friedman, Kostas Kokkotas, Shin Yoshida and Ewald Müller for helpful discussions and comments on the manuscript. All computations have been performed on a NEC SX-5/3C Supercomputer at the Rechenzentrum Garching. AG thanks the Max-Planck-Institut für Gravitationsphysik, Golm and the Max-Planck-Institut für Astrophysik, Garching, for supporting a visit during which this collaboration was initiated. This research was supported in part by the European Union grant HPRN-CT-2000-00137.

REFERENCES

Alcubierre M., Brügmann B., Dramlitsch T., Font J. A., Papadopoulos P., Seidel E., Stergioulas N., Takahashi R., 2000, Phys. Rev. D, 62, 044034
Banyuls F., Font J. A., Ibáñez J. M., Martí J. M., Miralles J. A., 1997, ApJ, 476, 221
Cheng K. S., Dai Z. G., 1998, ApJ, 492, 281
Clement M. J., 1981, ApJ, 249, 746
Clement M. J., 1984, ApJ, 276, 724
Clement M. J., 1986, ApJ, 301, 185
Colella P., Woodward P. R., 1984, J. Comput. Phys., 54, 174
Datta B., Hasan S. S., Sahu P. K., Prasanna A. R., Int, 1998, J. Mod. Phys. D, 7, 49
Dimmelmeier H., Font J. A., Müller E., 2001, in Ferrari V., Miller J., Rezzolla L., eds, ICTP Lecture Notes Series, Gravitational waves: a challenge to theoretical astrophysics, in press
Donat R., Font J. A., Ibáñez J. M., Marquina A., 1998, J. Comput. Phys., 146, 58
Font J. A., 2000, Living Rev. Relativ., 3, 2
Font J. A., Stergioulas N., Kokkotas K. D., 2000, MNRAS 313, 678 (FSK)
Font J. A., Miller M., Suen W.-M., Tobias M., 2000, Phys. Rev. D, 61, 044011
Hartle J. B., Friedman J. L., 1975, ApJ, 196, 653
Kokkotas K. D., Schmidt B. G., 1999, Living Rev. Relativ., 2, 2
Kokkotas K. D., Apostolatos Th., Andersson N., 2001, MNRAS, 320, 307
Lockitch K. H., 1999, PhD thesis, Univ. Wisconsin
Lockitch K. H., Friedman J. F., 1999, ApJ, 521, 764
Lockitch K. H., Andersson N., Friedman J. F., 2001, Phys. Rev. D, 63, 024019
McDermott P. N., Van Horn H. M., Scholl J. F., 1983, ApJ, 268, 837
Mönchmeyer R., Schäffer G., Müller E., Kates R. E., 1991, A&A, 246, 417
Ruffert M., Janka H.-Th., Schäfer G., 1996, A&A, 311, 532
Shibata M., Baumgarte Th. W., Shapiro S. L., 2000, Phys. Rev. D, 61, 044012
Shibata M., Uryu K., 2000, Phys. Rev. D, 61, 064001
Stergioulas N., 1998, Living Rev. Relativ., 1, 8
Stergioulas N., Font J. A., 2001, Phys. Rev. Lett., 86, 1148
Stergioulas N., Friedman J. L., 1995, ApJ, 444, 306
Stergioulas N., Font J. A., Kokkotas K. D., 2000, in Paul J., Montmerle T., Ausbourg E., eds, Proc. 19th Texas Symp. on Relativistic Astrophysics. Elsevier Science CD-ROM Series
Unno W., Osaki Y., Ando H., Saio H., Shibahashi H., 1989, Non-radial Oscillations of Stars. Univ. Tokyo Press, Japan
Wilson J. R., Mathews G. J., Marronetti P., 1996, Phys. Rev. D, 54, 1317
Yoshida S., Eriguchi Y., 2001, MNRAS, 322, 389
Zwerger T., Müller E., 1997, A&A, 320, 209

This paper has been typeset from a TEX/LATEX file prepared by the author.